

X-ray Outburst in Mira A

Margarita Karovska¹, Eric Schlegel¹, Warren Hack², John Raymond¹, and Brian E. Wood³
Harvard-Smithsonian Center for Astrophysics, 60 Garden Street, Cambridge, MA

ABSTRACT

We report here the Chandra ACIS-S detection of a bright soft X-ray transient in the Mira AB interacting symbiotic-like binary. We resolved the system for the first time in the X-rays. Using Chandra and HST images we determined that the unprecedented outburst is likely associated with the cool AGB star (Mira A), the prototype of Mira-type variables. X-rays have never before been detected from an AGB star, and the recent activity signals that the system is undergoing dramatic changes. The total X-ray luminosity of the system is several times higher than the luminosity estimated using previous XMM and ROSAT observations. The outburst may be caused by a giant flare in Mira A associated with a mass ejection or a jet, and may have long term consequences on the system.

Subject headings: binaries: symbiotic— stars: activity — stars: AGB and post-AGB — stars: Individual (Mira AB)— stars: winds, outflows — X-Rays: general

1. Introduction

Mira AB is an interacting binary system composed of an aging cool giant (Mira A) losing mass at a rate of $\sim 10^{-7} M_{\text{sol}}/\text{yr}$ (Bowers & Knapp, 1988), and an accreting companion (Mira B) about ~ 70 AU ($\sim 0.6''$) away. This detached binary is one of very few wind accreting systems that has been spatially resolved and for which the energy distribution of both components can be determined *unambiguously* (Karovska *et al.*, 1997). Studies of Mira AB wind accretion and mass transfer at wavelengths ranging from X-rays to radio pro-

vide a basis for understanding wind accretion processes in many other astronomical systems that currently cannot be resolved. Therefore this nearest symbiotic-like system offers a test-bed for detailed studies of wind accretion processes and accretion theory (Livio 1988).

In 1995, using the HST FOC, we resolved the system for the first time spatially and spectrally at UV and optical wavelengths and studied the interacting components individually (Karovska *et al.* 1997). In the past few years we have been witnessing changes in the spectral energy distribution (SED) of Mira AB, especially in UV (Karovska *et al.* 1997; Wood, Karovska, & Hack 2001). In addition to the general fading of the accretion luminosity, another baffling development was the appearance of a forest of Ly α -fluoresced H₂ emission lines, which dominated the HST spectra in 1999, despite not being seen at all in the 1995

¹Harvard-Smithsonian Center for Astrophysics, 60 Garden Street, Cambridge, MA

²Space Telescope Science Institute, Baltimore, MD 21218.

³JILA, University of Colorado and NIST, Boulder, CO 80309-0440.

spectra or by IUE (Wood, Karovska, & Hack 2001; Wood, Karovska, & Raymond, 2002). A similar drop in the accretion luminosity and appearance of a set of Ly α -fluoresced H₂ emission lines were also seen in the FUSE spectra in 2001 (Wood & Karovska 2004). Variable mass loss from Mira A could have caused the changes in the UV flux of Mira B observed in the past 10 years signaling that the system is undergoing dramatic changes.

In 1993, the *ROSAT* observation of Mira AB resulted in the first unambiguous detection of X-ray emission from Mira AB (Karovska et al. 1996). This observation resolved the contradicting results from the analysis of the *EINSTEIN* observation; Jura & Helfand (1984) marginally detected an X-ray source, while Maggio et al. (1990) set an upper limit of $f_x < 1.4 \times 10^{-13}$ erg s⁻¹ cm⁻². The *ROSAT* X-ray luminosity of the Mira AB system was estimated $\sim 10^{29}$ erg s⁻¹ (Karovska et al. 1996) which is similar to the luminosity estimated from the XMM observations carried out about ten years later (Kastner & Soker 2004b).

In this *Letter* we report the initial results from our recent Chandra observations and from coordinated HST and ground-based observations of Mira AB, including our discovery of a soft X-ray outburst in Mira A.

2. Observations and Analysis

On 2003 December 6 we carried out a 70 Ksec pointed Chandra observation of Mira AB using the ACIS-S instrument (Weisskopf *et al.* 2002). The source was placed at the nominal aim point of ACIS-S, on CCD S3. We analyzed the *Chandra* observations using *CIAO* data reduction and analysis routines.¹ The source spectrum was extracted using an aper-

¹CIAO is the Chandra Interactive Analysis of Observation's data analyses system package (<http://exc.harvard.edu/ciao>)

ture of 12'' radius centered on Mira AB; the background came from a surrounding annulus of inner radius 14'' and outer radius 30''. Figure 1 shows the Chandra spectrum and the best spectral fit (described in detail in §3.2). The source contained 5115 counts for a count rate of 0.073 ± 0.001 cts s⁻¹. The background rate was 0.0007 cts s⁻¹. In the 0.2-0.7 keV band, the count rate was 0.066 ± 0.001 cts s⁻¹ (background: 0.0003 cts s⁻¹); in the 0.7-4 keV band, the detected rate was 0.008 cts s⁻¹ (background: 0.0004 cts s⁻¹). The combination of the declining effective area below 0.5 keV plus the excess absorption layer (Chandra Proposer's Guide²) ensure minimal or zero photon pile-up. Pushing all of the model parameters to their most pile-up-favorable extremes yields a pileup estimate of less than 4%.

We detected several thousand counts below 1 keV associated with a new bright soft source in the system, which was not reported a few months before by XMM (Kastner & Soker, 2004b), or by ROSAT in 1993 (Karovska et al., 1996). The high-energy component (>1keV) is similar in appearance to the quiescent XMM and ROSAT spectra. However, a detailed comparison shows that a clear evolution has occurred in this portion of the spectrum (~ 1.2 -1.8 keV) as well. The count rates (see below), if folded through the XMM or ROSAT effective areas, would have been easily detected in either instrument. Furthermore, the spectrum is dominated by the soft component in the 0.2-0.7 keV band and the spectral behavior of the ROSAT and XMM spectra is significantly harder.

Following the Chandra X-ray outburst detection, we requested and obtained Director's time on Chandra and HST. Chandra HRC/LETG observations (40 Ksec) were carried about two months after the initial Chan-

²<http://asc.harvard.edu/proposer/POG/index.html>

dra observations (on January 11 2004). We detected signal only in the zeroth order of the spectrum which showed that the brightness of the soft source had dropped significantly. This observation detected ~ 80 counts. Were the soft ACIS spectral component (§3.2) still present with the same absorbed flux at the time of the LETG observation, >250 counts would have been detected in the zero-order image. However, the detected counts could be due to the hard source as well, or to both sources. Further modeling using the HRC and the ACIS observations is in progress.

We carried out follow-up HST STIS CCD and MAMA observations about two months after the initial Chandra observations (2004 February 2 and February 16). We resolved the system in the near-UV and obtained individual spectra of both components. MultiDrizzle techniques (Koekemoer et al. 2002) were used to combine multiple CCD images recorded using the F28x50OII filter centered on the [OII] 3729 Å line. The images resolved the system and detected extended emission. The STIS spectra show a significant increase in the Mg h & k lines emission in Mira A and in Mira B when compared to the 1999 STIS observations. Velocity shifts of the order of 100 km/s were also detected in Mira A's Mg h & k lines. A similar increase of line emission was detected in the optical spectra (H_α and OIII λ 5007Å lines) obtained at the Oak Ridge observatory. In addition, broadening and complex structure were observed in the H_α during the month following the X-ray outburst, indicating velocities of ~ 100 km/s. Further details of the analysis and the results of the Chandra, HST, and ground-based observations will be discussed elsewhere (Karovska *et al.*, 2005, in prep.).

3. Results

3.1. X-ray and near-UV Imaging

The ACIS-S raw image of Mira AB binned at the detector 0.495" pixel resolution showed an elongation along the Mira AB system axis (Figure 2a). We made soft (< 0.7 keV) and hard (0.7-2 keV) images of Mira AB, filtered based on the major components detected in the ACIS-S spectrum. Figure 2b shows the image of the hard source (to the East) with an overlay of the contours of the soft component (to the West). The centroids of these sources are displaced by $\sim 0.6''$.

We attempted to do further spatial analysis using the HRC zeroth order image. The image appears extended and it is shifted ~ 0.3 arcseconds from the soft ACIS image, in the direction toward the hard ACIS image. It could therefore be associated with Mira A or Mira B (or both). However, the low counts and lack of spectral resolution make it difficult to determine if there is a component associated with a remnant of the outburst. Although the HRC pixels ($\sim 0.14''$) are indeed smaller than the ACIS pixels, the actual resolution of the HRC is in fact comparable to ACIS. Furthermore, there are additional artifacts in the HRC images that makes it very difficult deciding if the extension in the image to the South and an additional source 0.5" to the West are real.

We explored the spatial extent of the emission in the ACIS-S (0.3-4 keV) image of the system at 0.2" resolution using a new multiscale deconvolution technique *EMC2* (Esch *et al.* 2004) and *Chandra* PSF model. This was possible because the *Chandra* data include information about the photon energies and positions which was used to obtain filtered images and carry out sub-pixel resolution analysis. The *Chandra* PSF varies as a function of energy and off-axis angle; we carried out PSF simulations using CIAO software

and threads, including the ChaRT PSF simulator³. The PSF simulation was carried out using information on the spectral distribution and off-axis location of the system as inputs to ChaRT. The *EMC2* deconvolution technique, described in detail in Esch *et al.* 2004, was developed for low-count statistics data, and it provides error estimates in addition to the reconstructed images.

The deconvolved image (color image in Figure 3) shows two sources separated by $\sim 0.6''$. The pixel size is $0.1''$ (0.2 ACIS-S pixel size). This is the first image of an interacting binary that has been spatially resolved at X-ray wavelengths. We note that the location of the brighter source in the deconvolved image (to the West) corresponds to the position of the soft source (as determined using filtered ACIS-S images), and the fainter source (to the East) corresponds to the hard-band ACIS-S image.

We compared the X-ray images with the HST images of the Mira AB components obtained two months later, showing two sources separated by $\sim 0.6''$. In the HST images Mira A is to the west of Mira B. Figure 3 displays the overlay of the contours of the HST 3729 Å image on the Chandra deconvolved image, showing that the soft X-ray source is in the vicinity of the of Mira A. The soft source is therefore likely associated with the AGB star rather than with the accreting companion Mira B. When the X-ray image is compared to the HST image of Mira A and Mira B, we see slightly larger separation of the X-ray components ($\sim 0.1''$) and possible small rotation of the axis between the sources. This difference could be real, but also it could be due to uncertainties in the deconvolution, or to the limited resolution in the Chandra data. It could also be a result of HST absolute positioning uncertainties.

³<http://asc.harvard.edu/chart/index.html>

The X-ray images of Mira A and Mira B appear extended. Furthermore, the Chandra image shows a faint “bridge-like” feature extending between the components. Similar “bridge-like” structure was detected in the 1995 HST images indicating possible mass flow between the components (Karovska *et al.* 1997). Although the features in the X-ray image are uncertain because of the low count level and/or possible PSF and deconvolution artifacts, we note that very similar structures can be seen in the overlaid HST contours.

We determined that some of the extended structure in the HST image to the right of Mira A, in the opposite direction from Mira B, is due to an undocumented red leak of the F28x50OII filter. Following the HST observations we discovered and confirmed the red leak in other very red sources. For example, F28x50OII filter images of CH Cyg, which contain a very red component, show similar structure, and we have detected similar structured PSF in the [OIII]5007 filter during the 1999 observation of Mira AB.

The evidence of extended structures in both components in both X-ray and UV images is uncertain and require further analysis and modeling. In order to determine if there was a mass ejection during the outburst, it will be necessary to carry out further high-angular resolution monitoring including at X-ray and UV wavelengths.

3.2. X-ray Spectroscopy

The spectrum was binned to a minimum of 20 counts per channel. The effective area was corrected for the energy- and time-dependent instrumental absorption and *Xspec* v11.0 was used to fit the spectra (Arnaud 1996) as detailed below. The X-ray spectrum shows strong soft emission and potentially multiple harder components. Standard continuum models (bremsstrahlung, blackbody, power law) did not provide good fits to the soft com-

ponent. We describe the spectral fit below with 90% errors on the model parameters.

We fit the low-energy portion of the spectrum using an absorbed model spectrum consisting of a sum of gaussians, each with a fixed center and zero width to represent an un-resolved line. We included several C, N, and O lines. The line centers (in keV) are at C V 0.299, 0.304, 0.308; C VI 0.367; N VI 0.319, 0.426, 0.431; C VI 0.435, 0.459; N VII 0.500; O VII 0.561, 0.569, 0.574; and O VIII 0.653). For each line, only the normalization was fit. The initial fit showed that the O line normalizations were all consistent with zero as were approximately half of the C and N normalizations; a subsequent fit used a model containing only the C and N lines. Figure 1 shows the result with lines at C VI 0.367 keV, N VI 0.426 keV, C VI 0.459 keV, and N VII 0.500 keV (line normalizations = 4.9, 6.2, 50.8, and 33.1, respectively, in units of 10^{-5} photons cm^{-2} s^{-1}). Because of the limited spectral resolution we cannot determine if there are any specific lines detected, or if the fit is unique. When we added a continuum component, its model normalization was consistent with zero. The apparently large residuals near 0.3 keV may be explained by the known problems with the corrections for the contaminant near the carbon edge (Marshall 2003⁴). The best-fit spectrum is therefore most easily explained as blended emission of C + N lines.

The hard component was best-fit with a bremsstrahlung continuum of $kT \sim 0.78^{+0.15}_{-0.23}$ keV to mimic an optically thin thermal plasma, plus two zero-width gaussians representing emission lines at $1.02^{+0.06}_{-0.04}$ and $1.36^{+0.03}_{-0.04}$ keV, all absorbed by a column $N_{\text{H}} \sim 9.0^{+0.15}_{-0.12} \times 10^{22}$ cm^{-2} . Other models provided very poor fits including models containing additional gaussians at the posi-

tions of expected line emission. The fitted bremsstrahlung temperature is nearly identical with the value determined from the XMM spectrum (Kastner & Soker 2004b). The fitted column is about a factor of two higher than the XMM-determined value. A specific error range is not shown for the XMM value, but the authors state “formal uncertainties are $\approx 20\%$ ”. A 20% error range on the XMM value places it outside the 90% range of the fitted value determined here suggesting the column may have increased by a factor of ≈ 2 between the two observations. The hard gaussians have equivalent widths of 236^{+244}_{-110} and 124^{+124}_{-50} eV, respectively, and we attribute them to Ne and Mg emission lines. We note, Ne IX and Ne X lines were also detected by the XMM (Kastner & Soker 2004), but the Mg line is not pronounced in the XMM spectrum. These results are similar to the enhanced $K\alpha$ H-like Ne and He-like Mg lines observed in the ASCA spectrum of the symbiotic CH Cyg showing jet activity (Ezuka et al. 2001), corresponding to $\log(T)=6.8$. Our signal-to-noise is insufficient to fit for the He-like Si line (found in the CH Cyg spectrum). These high temperature lines may indicate shock heated emission or could be associated with the flare or a jet-like ejecta.

We calculated the total flux from the system 5.6×10^{-13} (0.2-4 keV), 5.5×10^{-13} (soft component only in 0.2-0.7 keV), and 2.7×10^{-14} (hard component only in 0.7-4 keV) $\text{erg s}^{-1} \text{cm}^{-2}$ for the bands defined. The unabsorbed fluxes are very sensitive to the adopted column. The fitted column toward the soft source is $\sim 8.0 \times 10^{19} \text{cm}^{-2}$. This value, if adopted as the column *toward the system*, is not consistent with the column obtained from the ROSAT spectrum (Karovska et al. 1996) nor the XMM observation (Kastner & Soker 2004b). However, the fitted column is really only a lower limit. The 90%

⁴Available at http://space.mit.edu/ASC/calib/letg_acis/ck_cal.conf. Confidence contour is closer to $\sim 2.8 \times 10^{20}$

cm⁻². Within this upper limit, the column remains inconsistent with the XMM value, but is consistent with the column determined from the UV H₂ line spectroscopy (Wood et al. 2002). If we adopt the formal-fit column from the soft spectrum, then the unabsorbed fluxes are 6.4×10^{-13} (0.2-4 keV), 6.2×10^{-13} (0.2-0.7 keV), and 2.7×10^{-14} (0.7-4 keV) erg s⁻¹ cm⁻². If we adopt the upper limit value for the column, the unabsorbed fluxes are 8.3×10^{-13} (0.2-4 keV), 8.0×10^{-13} (0.2-0.7 keV), and 2.7×10^{-14} (0.7-4 keV) erg s⁻¹ cm⁻². Adopting the fitted value of the column for the hard component, the unabsorbed hard band flux is 9.9×10^{-14} erg s⁻² cm⁻² (0.7-4 keV).

We emphasize that the appropriate N_H value could be completely different for the hard and soft sources since the emissions originate from different places. It is conceivable that a persistent low energy X-ray source exists, and that it was made visible by a temporary drop in the neutral column density surrounding Mira A. It seems more likely, however, that an X-ray flare ionized its surroundings, producing the formal value of smaller column as a side effect. Taking note of the different columns toward the sources, the unabsorbed luminosity then falls into the range of $1.5\text{-}2 \times 10^{30}$ erg s⁻¹, for an assumed distance of 130 pc, and assuming the luminosity is the sum of the soft and hard components separately. The range results from the adopted value of the column toward the soft component. The total luminosity is about a factor of 2-4 higher than that observed by XMM and ROSAT. A detailed analysis and modeling of the *Chandra* data combined with the multi-wavelength observations of the outburst will be discussed elsewhere (Karovska *et al.*, 2005, in prep.).

4. Possible Causes and Consequences of the X-ray Outburst

Detecting X-ray emission from Mira A is a very important result because X-ray emission has not been detected so far in single AGB stars, including Miras (e.g. Kastner & Soker 2004a). The soft X-ray outburst in Mira A could be caused by a magnetic flare followed by a large mass ejection, analogous to the solar flares and Coronal Mass Ejections (CMEs). Soker and Kastner (2003) suggested that magnetic reconnection events near the stellar surface should lead to localized, long-duration flares. The crude time scale for a flare might be estimated by multiplying the 1-2 day time scale for a large flare on an RS CVn star by the ratio of Mira A's radius (few hundred solar radii) to that of the RS CVn star (4-15 solar radii), suggesting time scales from weeks to months, which is in accordance with the time scale of the X-ray event observed by Chandra.

In the case of mass ejection we could expect changes in the SED of both components on a time scale of months to years. As the ejected material cools down we expect a significant increase in dust formation in the system in 2004/2005. This is also the time scale on which we would expect a response of the accretion disk around Mira B to any disturbance caused by an outburst on Mira A in late 2003, if the flow is propagating toward Mira B with speed of \sim hundred km/s (as suggested by our preliminary analysis of the HST and ground-based spectroscopy). An increased outflow from Mira A resulting from the recent outburst could help renew the accretion disk around the companion, following the low-state observed by HST and FUSE in 1999–2001.

The increased accretion rate into Mira B could also cause instabilities in the accretion disk and jet-like activity (e.g. Soker 2002) similar to that detected in several nearby

unresolved symbiotic systems (e.g. in CH Cyg, Corradi et al. 2001, R Aqr, Kellogg et al. 2001). An outburst in Mira B associated with the accretion disk instabilities could be analogous to a dwarf nova outburst except that the much larger size of the wind-fed disk in this well-separated binary would increase the duration from about a week to many months. Further multiwavelength observations are necessary to determine the nature and characteristics of instabilities in the system and/or its individual components that may have caused the outburst, and to understand the long-term consequences of this outburst on the system.

We are grateful to Drs H. Tananbaum and S. Beckwith for granting Director's time on Chandra and HST. This work is part of a long term collaboration with several colleagues on coordinated multi-wavelength campaign including Drs. R. Stefanik, M. Marengo, J. Drake, A. Henden, D. Esch, L. Matthews, E. Guinan, E. Waagen and the AAVSO. We dedicate this paper to Janet A. Mattei who has inspired this work and made these observations possible for many years. We thank the referees N. Soker and J. Kastner for helpful suggestions. This work was supported by NASA grants GO4-5024A and NAS8-39073. MK and ES are members of the Chandra X-ray Center, which is operated by the Smithsonian Astrophysical Observatory under contract to NASA NAS8-39073.

REFERENCES

- Arnaud, K.A., 1996, ADASS V, Vol. 101, 1996, G. H. Jacoby & J. Barnes, eds., p. 17.
- Bowers, P.F. & Knapp G.R, 1988, ApJ, 332, 299.
- Corradi R.L.M. *et al.*, 2001, ApJ, 560, 912.
- Esch, D.N., Connors, A., Karovska, M., & van Dyk, D.A., 2004, ApJ, 610, 1213.
- Ezuka, H., Ishida, M., & Makino, F. 1998, ApJ, 499, 388.
- Jura, M., & Helfand, D.J, 1984, ApJ, 287, 785.
- Karovska, M., Raymond, J., & Guinan, E. 1996, SAO Tech Report, Cambridge, SAO.
- Karovska, M., Hack, W., Raymond, J., & Guinan, E. 1997, ApJ, 482, L175
- Kastner, J.H., & Soker, N., 2004a, ApJ, 608, 978.
- Kastner, J.H., & Soker, N., 2004b, ApJ, 616, 1188.
- Kellogg, E., Pedelty, J., and Lyon, R. 2001, ApJ, 563, L151.
- Koekemoer, A. et al., 2002, in "HST Calibration Workshop", p. 337
- Livio, M. 1988, in Symbiotic Phenomena, Proceedings of IAU Coll. No . 103.
- Maggio, A. et al. 1990, ApJ, 348, 253.
- Soker, N., 2002, MNRAS, 337, 1038.
- Soker and Kastner 2003, ApJ, 592, 498.
- Weisskopf, M.C. *et al.*. 2002, PASP, 114, 1.
- Wood, B.E., Karovska, M., & Hack, W. 2001, ApJ, 556, L51.
- Wood, B.E., Karovska, M., and Raymond, J.C. 2002, ApJ, 575, 1057.
- Wood, B.E., and Karovska, M., 2004, ApJ, 601, 502.

This 2-column preprint was prepared with the AAS L^AT_EX macros v5.2.

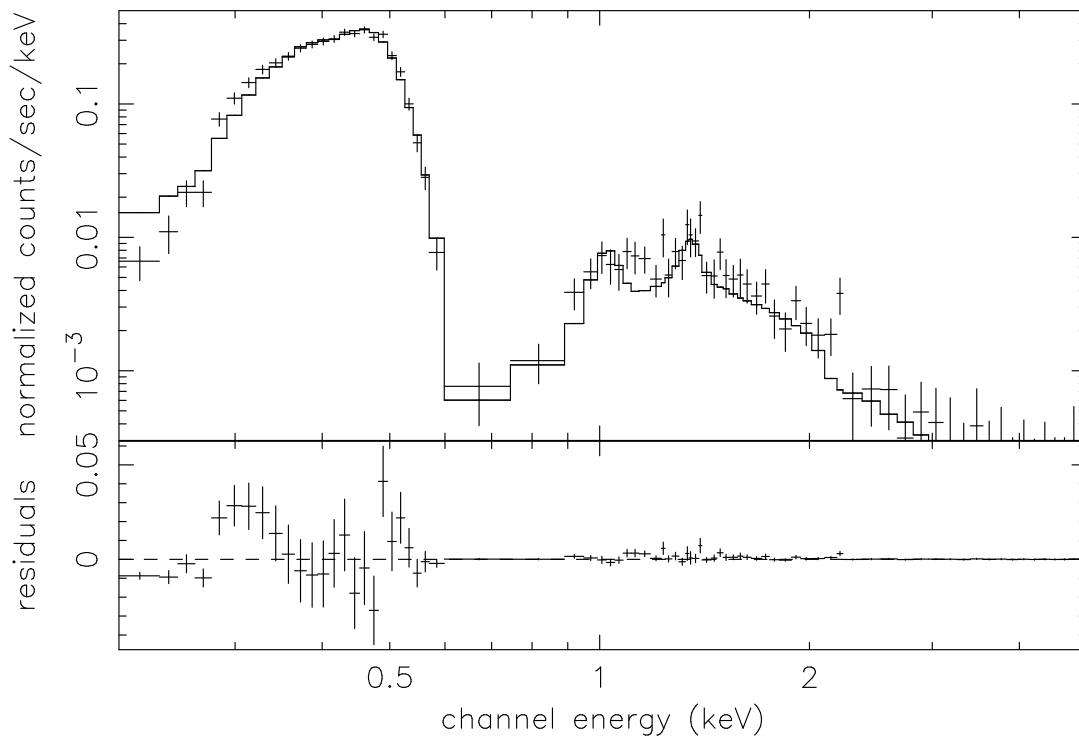


Fig. 1.— *Chandra* ACIS-S spectrum of Mira AB (plus signs) fit with a combination of gaussians for the soft spectral component and a bremsstrahlung plus gaussians for the hard component (see §3.2). Residuals fall mostly near the C edge at 0.3 keV where the response matrix is known to have errors.

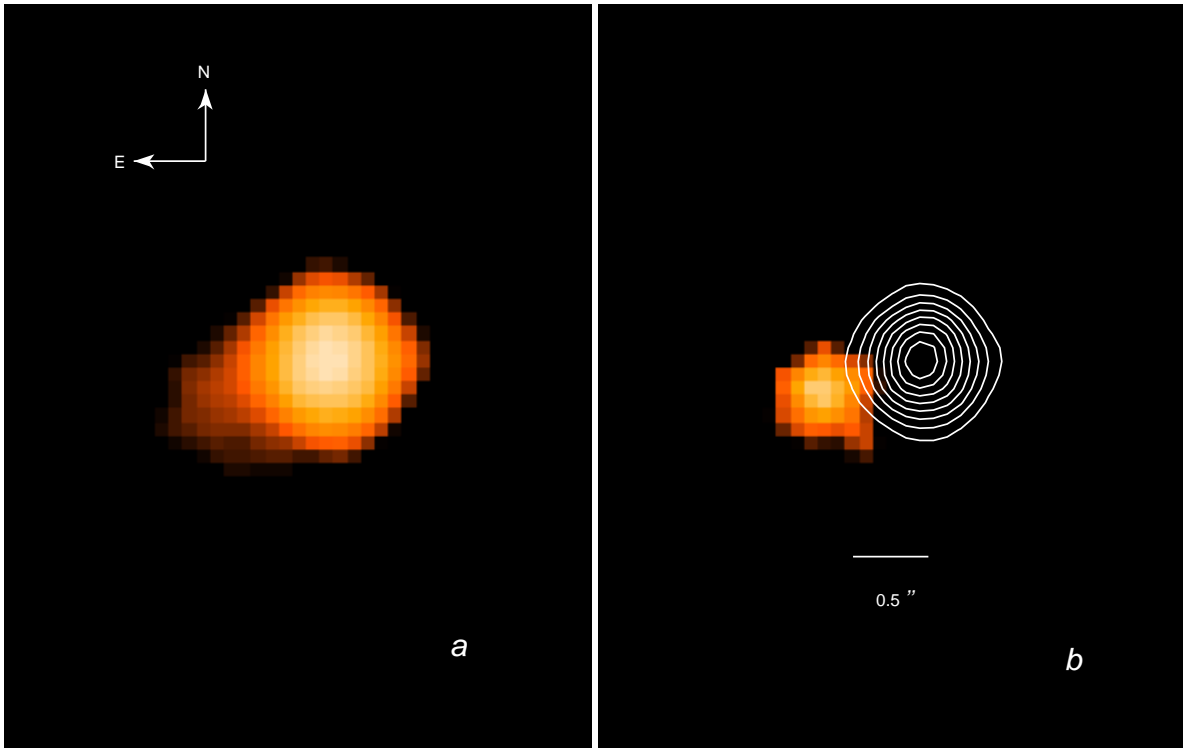


Fig. 2.— *Chandra* images of Mira AB: (a) ACIS-S raw image of Mira AB filtered from 0.3 to 2 keV. Mira A is toward the West (see Fig. 3); (b) contours of the ACIS-S soft image (0.3-0.7keV) (toward the West) overlaid on the image of the hard image (0.7-2 keV) (toward the East).

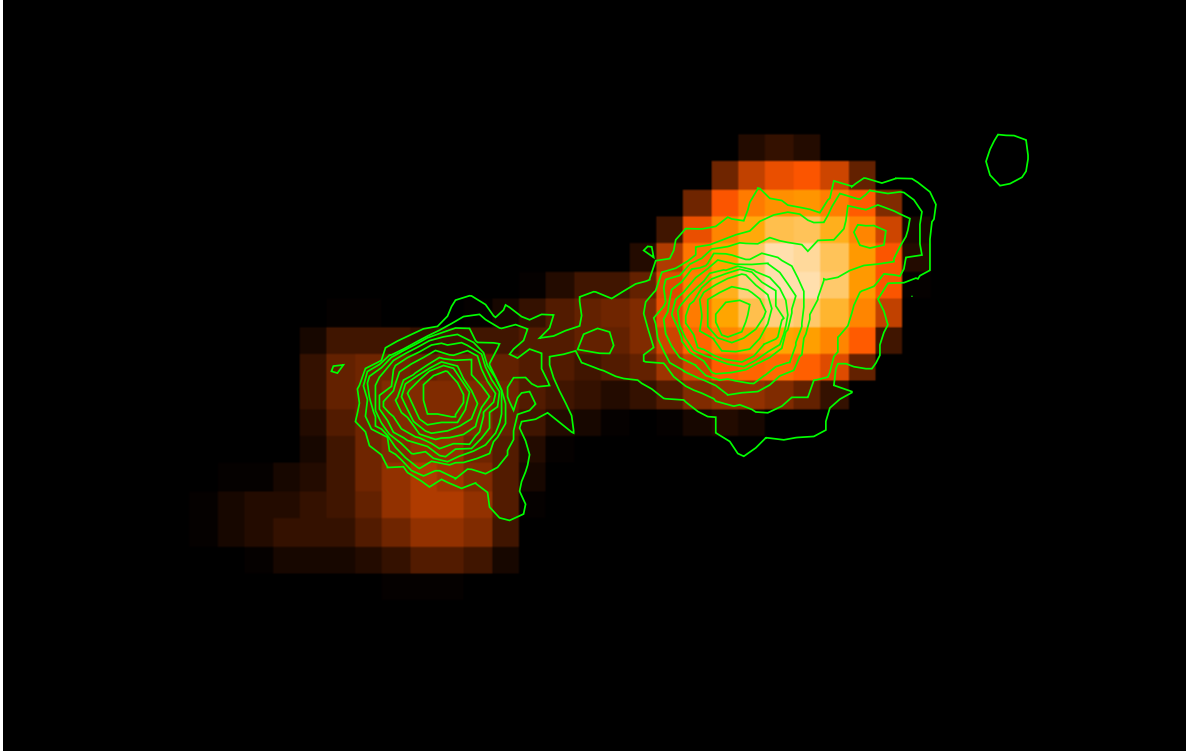


Fig. 3.— *Chandra* image of Mira B (left) and Mira A (right), separated by $\sim 0.6''$, with overlaid contours of the HST 3729 Å image of the system. North is up, East is to the left. The apparent extended point-like structures in the HST contours of Mira A in the NW direction are PSF structures due to a red leak in the filter.